Out of Africa by spontaneous migration waves

Paul D. Bons[1*], Catherine C. Bauer[1,2]. Hervé Bocherens[1,2], Tamara de Riese[1], Dorothée G. Drucker[1,2], Michael Francken[1,2], Lumila Menéndez[1,3], Alexandra Uhl[4], Boudewijn P. van Milligen[5], Christoph Wißing[1]

[1] Department of Geosciences, Eberhard Karls University Tübingen, Tübingen, Germany

[2] Senckenberg Centre for Human Evolution and Palaeoenvironment (HEP), Tübingen, Germany

[3] Departamento de Antropología, Universidad Nacional de La Plata, La Plata, Argentina

[4] Department of Anthropology, Boston University, Boston, Massachusetts, United States of America

[5] National Fusion Laboratory, CIEMAT, Madrid, Spain

* Corresponding author

paul.bons@uni-tuebingen.de

Abstract

Hominin evolution is characterized by progressive regional differentiation, as well as migration waves, leading to anatomically modern humans that are assumed to have emerged in Africa and spread over the whole world. Why or whether Africa was the source region of modern humans and what caused their spread remains subject of ongoing debate. We present a spatially explicit, stochastic numerical model that includes ongoing mutations, demic diffusion, assortative mating and migration waves. Diffusion and assortative mating alone result in a structured population with relatively homogeneous regions bound by sharp clines. The addition of migration waves results in a power-law distribution of wave areas: for every large wave, many more small waves are expected to occur. This suggests that one or more out-of-Africa migrations would probably have been accompanied by numerous smaller migration waves across the world. The migration waves are considered "spontaneous", as the current model excludes environmental or other factors. Large waves preferentially emanate from the central areas of large, compact inhabited areas. During the Pleistocene, Africa was the largest such area most of the time, making Africa the statistically most likely origin of anatomically modern humans, without a need to invoke additional environmental or ecological drivers.

Introduction

Hominins are generally supposed to have originated in Africa and settled most of Africa and the southern half of Eurasia in the early Pleistocene [1-5]. Fossil evidence suggests that earliest *Homo sapiens* appeared in Africa during the late Middle Pleistocene (Jebel Irhoud, Omo and Herto [6-8]). Anatomically modern humans (AMH) emerged, spread out of Africa during the Late Pleistocene and now occupy the whole world as the only *Homo* species [9-13]. In the intervening time, a number of *Homo* species, such as Neanderthals, Denisovans, *Homo erectus*, *H. heidelbergensis*, *H. ergaster*, etc. existed, developed and disappeared again [14-21]. Pleistocene human evolution is thus characterised by differentiation, speciation, migration waves and extinction events. Most authors assume that the out-of-Africa spread of AMH involved one or more migration waves that replaced *Homo* species that existed at the time with only limited genetic admixture, such as between Neanderthals and AMH [22-23]. Many studies have addressed the timing and origin of migration waves, as well as migration paths [e.g. 24,22,25,26,13]. Apart from the major out-of-Africa event(s), AMH populations experienced several more migration waves within already populated areas, such as Africa [27-28] and Europe [29-30]. Considering this, it is not unlikely that more migration waves occurred in the Pleistocene, but the sparse fossil record still makes it difficult to detect any.

Assuming that migration waves did happen, the question arises what caused them, in particular the spread of AMH. Most authors favour some competitive advantage of AMH over other *Homo* species [31-33]. With climate change now central in the scientific discourse, many recent studies suggest that climate played an important role in the environmental changes making AMH more competitive than other *Homo* species, or allowing opening ecological corridors for dispersal of *Homo sapiens* out of Africa [34-42].

An opposite view is that AMH and Neanderthals actually had no competitive advantage over each other [43]. The argument, based on a numerical model, is that, because AMH's population was much larger than that of Neanderthals [44-46,12], AMH's were statistically more likely to reach fixation in both Africa and Europe.

Although modelling is extensively used in studies of human evolution [e.g. 47-48], relatively few studies so far employed forward approaches on an explicit map to, for example, determine amounts of admixture, stepping stones or the most probably origin of AMH [49,50,38,51,52,43]. Kolodny and Feldman [43] used a simple "map" with only two demes to determine the chances that AMH would replace Neanderthals purely due to the larger population of AMH in Africa compared to Neanderthals in Europe. The SPLATCHE2 simulations [52] and the similar model by Eriksson et al. [38] assumed *a priori* that AMH have some advantage and explored the advance of AMH in relation to climate factors. These various models have in common that the species (AMH) and its competitive advantage are predefined.

Here we present a basic numerical model to simulate the spatial and temporal differentiation/speciation and the emergence, frequency and patterns of migration waves. Contrary to the above-mentioned models, no human species are defined *a priori*. The only aim is to explore the statistics of patterns, without claiming or attempting to simulate the actual emergence and spread of AMH, which would only be one of an infinite number of realisations of the stochastic model. Although a range of environmental factors have been invoked to explain various aspects of human evolution, we expressly do not include these in the models presented here. The aim is to provide a null hypothesis against which additional environmental factors and influences can be further tested.

Methods

The model is based on a regular 2-dimensional grid of demes, each a square area with a number of individuals. The genome (G) of a deme is defined by a single string of N binary genes, with two alleles, either zero or one (similar to e.g. [53]. This genome is the single dominant or representative genome for the population of a deme. The temporal and spatial evolution of genomes is modelled in discrete time steps of length Δt in which mutations take place and genes are transferred between neighbouring demes. The distribution of genomes is visualised in RGB colour maps in which each deme is one pixel. Red is proportional to the number of ones in the deme's genome, blue proportional to the number of genes identical to Gi={10101010, etc.} and green proportional to the number of genes identical to Gi={00110011, etc.}. Colours are stretched to maximise the colour range.

Mutations

Mutations are carried out at the start of each time step. For each mutation, a deme is first randomly picked. Next, a random gene that has allele "0" everywhere in the model is chosen. This gene will be mutated by changing its allele from "0" to "1" in the deme. This procedure is repeated M times (the mutation rate) per time step. The mutation chance (m) per time step for one single deme is $m=M/A$, with A the area of the model. m is the chance that one mutation emanating from a single individual reaches fixation in the whole population (of

size N_D) of a single deme in a time step of T generations. m thus depends on T, N_D (itself the product of population density ρ and area S^2 of a deme) and the intrinsic mutation rate m_0 of one individual per generation. The number of mutations that occur in one deme per generation is proportional to $N_D \cdot m$. However, the chance that a mutation reaches fixation within the population is roughly inversely proportional to N_D for $s \approx 0$, with s the competitive advantage [54]. It follows that the rate of successful mutations within the deme is proportional to m_0, and is not dependent on the population size of the deme. The model, however, uses time steps T of more than one generation. It will be shown below that $T \propto N_D$, and hence, $m \propto m_0 \cdot N_D$.

We use the term "active mutations" for those mutations that have not reached fixation, i.e. they occupy at least one, but not every deme in the map of all demes Once a mutation has reached fixation by occupying every deme in the model it no longer plays an active role. The timing of fixation of a mutation is recorded, as well as the location of origin of the mutation.

Allele exchange between neighbours

A mutation step is followed by one round of interbreeding in which single alleles may be transferred between neighbouring demes (here using a Von Neumann direct neighbourhood scheme). All demes are considered on average once in a random order for transfer between a deme (deme a) and a randomly selected direct neighbour (deme b). Each pair is thus treated every two steps on average. The chance that a transfer between neighbouring deme is considered in one time step is defined by the parameter D. It can be

regarded as a general diffusion parameter: the chance, per time step, that an allele jumps from one deme to a neighbour in a random Brownian movement [55-57,54]. Assortative mating [58] is included in a way similar to the model of Barton and Riel-Salvatore [51]. With assortative mating, similar individuals are more likely to mate than different ones. This is implemented with the "assortative mating factor" (α), which reduces D as a function of ΔG, which is the number of genes that have different alleles in the two neighbouring demes under consideration:

$$D = D_0(1 - \alpha\Delta G), \text{ with } \Delta G = \sum|G_{(a)} - G_{(b)}|. \quad (1)$$

D_0 is the reference diffusion parameter, equal to D for the case that α=0. It is first decided with a random-number generator whether a gene transfer will take place or not, according to Eq. (1). If this is to happen, all genes in the list are considered for allele transfer. The chance $P(a \rightarrow b)$ that an allele of the genome of deme a is copied to deme b is calculated with:

$$P\left(a \rightarrow b\right) = 0.5 + p\,\Delta F_{a,b}, \text{ with } \Delta F_{a,b} = \sum G_{(a)} - \sum G_{(a)} \text{ and } P(b \rightarrow a)=1-P(a \rightarrow b). \quad (2)$$

$\Delta F_{a,b}$ is the difference in number of mutations (ones) between the two demes. The chance that a deme passes on its mutations to a neighbour is thus determined by the overall number of mutations relative to that neighbour ($\Delta F_{a,b}$) and the advantage factor p that defines the competitive advantage of these mutations (assumed the same for all mutations). In this paper we define the sum of all genes ($F=\Sigma(G)$) as the "fitness" of a deme. This is because the number of advantageous genes (F), multiplied by the advantage factor (p) determines the chance that genes are passed on to offspring. When p=0, mutations are neutral and there is no preferential transfer of alleles and we have purely random

156 spreading of zeros and ones, but, on average, no change in their frequency. A positive value
157 of p leads to fitter demes to pass on their alleles to their neighbours. Note that the transfer
158 chance of a single allele does not only depend on its own value, but on that of the whole
159 genome. This can potentially lead to less competitive zeros replacing more competitive
160 ones.

161 To estimate the duration of one time step, we can consider the population of the two
162 neighbouring demes as one during the transfer. Of interest is the case where the mutation
163 only occurs in one of the two demes, i.e. when it is carried by 50% of the combined
164 population. The time step T (in number of generations) is thus the time it takes for a
165 mutation to reach fixation by genetic drift in the combined population with a chance of
166 0.5+p or extinction with a chance of 0.5-p. Using a basic Monte Carlo model for populations
167 of up to a few hundred individuals, we find for the time step T (S1 Methods Eq. S3):

168 $$T \approx 7\frac{\rho S^2}{D_0} = 7\frac{N_D}{D_0}. \qquad (3)$$

169 Here, S is the size of a deme and ρ the population density. Equation (3) only holds for
170 weakly competitive mutations (s<<1), small values of p, and no variation in population
171 density between demes. The factor p is related to s, the competitive advantage of the
172 mutation [59,55-57,54] (S1 Methods Eq. S2):

173 $$p \approx 0.29 \cdot \rho S^2 \Leftrightarrow s \approx 3.4\frac{p}{\rho S^2} = 3.4\frac{p}{N_D}. \qquad (4)$$

174 At a deme size of S=50 km and a population density of 0.01 individuals/km^2, T is about 175
175 generations (≈4000 years at 25 years/generation) for D_0=1 as used throughout this paper.
176 Using p=0.05 results in a competitive advantage of s≈0.7%.

177

Spreading of mutations

A single mutation in a field of demes without any other mutations has a chance of 0.5-p to disappear the first time an interbreeding event is considered with one of its neighbours. The initial survival rate is thus a function of p. The low initial survival rate is due to two factors. The first is a numerical effect that the width of diffusional front is less than can be resolved at the scale of the demes. The second is related to genetic drift [60-61], where the effective population (cluster of demes around the new mutation) is small and therefore the chance of survival smaller than when the mutation has spread over a large area.

Once a mutation has survived this initial nucleation phase by spreading over sufficient demes, the area occupied by the deme increases linearly with time. The expansion front is not sharp, but diffuse, in accordance with the diffusion-reaction model of [55]. The width of the diffusional front decreases with increasing p (Fig 1A-C) as the advantage factor becomes more important relative to the diffusional spreading. After the initial nucleation phase, the area (A_{mut}) occupied by the single mutation increases linearly with the square of time. We define the velocity (v, in deme size per time step) of the expanding front as the rate of increase in radius (r_{eq}) of an equivalent circle with area A_{mut}:

$$v = \frac{dr_{eq}}{dt} = \frac{d\left(\sqrt{A_{mut}/\pi}\right)}{dt}. \quad (5)$$

The spreading velocity ($v_{(p)}$) as a function of p is determined from 2500 simulations of an expanding mutation after a stable diffusive front has been established ($50<r_{eq}<150$ demes). $v_{(p)}$ is determined by the chance (proportional to p) that the mutation is copied to a deme without that mutations and the length (L_{if}) of the interface between demes with and

without that mutation. L_{if} is much larger than the circumference ($2\pi r_{eq}$) of the equivalent circle in case of a diffusive front. $L_{if}/2\pi r$ thus decreases with p and can be approximated with a power law (using a least-squares best fit, with r^2=0.99565; Fig 1D):

$$\frac{L_{if}}{2\pi r_{eq}} \approx 1.43 \cdot p^{-0.45}. \quad (6)$$

As a result, $v_{(p)}$ is approximately a power-law function of p (r^2=0.9993; Fig 1E):

$$v_{(p)}=D_0 \cdot 0.83 \pm 0.02 \cdot p^{0.54} \text{ deme/step}. \quad (7)$$

The exponent is slightly larger than 0.5 due to the fact that the spreading front becomes less fuzzy with increasing p. This means that demes at the front have fewer neighbours without the mutation when p is large than when it is small.

Fig 1. Spreading rates of mutations. Distribution of a single mutation originating from the centre of a circular model (R=100 demes) at the stage where the effective radius of the area occupied by the mutation is 60 demes. **A**. p=0.0125 at t=990. **B**. p=0.025 at t=720. **C**. p=0.05 at t=410. The effect of increasing p is an increase in spreading rate and a sharpening of the spreading front. **D**. Interface length divided by effective circle circumference versus drift factor in a double-log plot. Data approximately follow a power law. **E**. As a result, spreading velocity versus advantage factor also shows a power-law relationship. **F**. Distribution of six mutations seeded at the centre of the model (R=100 demes) at t=0. Colours show number of mutations on a deme from one (pink) to six (black).

The initial spreading velocity is higher when multiple mutations are placed in the centre of the model (Fig 1F). This is expected, because ΔF>1 in Eq. (2). However, the steady-state velocity of these mutations is the same when the diffusion front is wide enough (low

223 p). The explanation is that demes within this diffusive front mostly only have a low ΔF with
224 their direct neighbours and thus spread as fast as a single mutation. This implies that gene
225 surfing due to high ΔF is not effective during steady-state spreading of an ensemble of
226 mutations. However, when two different populations, with high ΔF, would suddenly come
227 into contact the mutation spreading effect is expected to be high.
228

229 ## Replacement events

230

231 Full genome transfers or replacement events are considered after the interbreeding step.
232 Again, all demes and one random direct neighbour are considered in a random order. A full
233 genome replacement is carried out if the absolute fitness difference $|\Delta F|$ is equal or greater
234 than a set critical fitness difference ΔF_{crit}. In that case, the full genome of the fittest deme is
235 copied to that of its neighbour. After one round where all demes and one random neighbour
236 are considered once for a replacement, the replacements may have led to new pairs that
237 exceed ΔF_{crit}. The routine is therefore repeated until $\Delta F<\Delta F_{crit}$ everywhere in the model.
238 When Δt is small, this semi-instantaneous spreading would be relatively fast (up to the
239 order of a km/yr, depending on the size of demes). However, we use this scheme here to be
240 able to track individual replacement "avalanches" within one time step. Contiguous areas
241 that experienced a full genome replacement are termed "sweeps" here. The time and area of
242 each sweep (A_{sw}) is recorded at the end of each time step, as well as a map of all demes that
243 experienced a genome replacement sweep.
244

245 ## Aims

The aim of this paper is to illustrate the main types of evolutionary behaviour that result from different combinations of diffusive spreading with competitive advantageous mutations, assortative mating and replacement waves. It is not our intention to systematically investigate and quantify the effect of each of the parameters. We therefore only present four representative cases, using a reference model with 3 square inhabited areas, connected by narrow isthmuses. The areas or "continents" are 100x100, 50x50, and 25x25 demes in size. In each individual simulation presented below we keep all parameters constant in space and time. This implies that any environmental factors that could affect the competitive advantage of individual mutations, their spreading rate, and the population density are kept constant in space and time. This serves the aim of this paper to investigate patterns that develop in the complete absence of any environmental or other external influences. We consider this as a fundamental preliminary step in order to further discuss diversification processes during human evolution.

Results and discussion

Diffusion effect

We first consider the case (Fig 2A) without genome replacements ($\Delta F_{crit}=\infty$) or assortative mating ($\alpha=0$). The mutation rate M is set to four mutations per time step and p is 0.05. Individual mutations spread leading to increasing variation in genomes within the model.

This is comparable to the geographic differentiation through isolation-by-distance as proposed for the reticulate or multiregional evolution model [62-63] or the recent assimilation model [64-65]. Demes in the centre of the model are on average nearer to the origins of mutations than are demes on the periphery. Fitness therefore increases faster in the centre than the periphery, as can be seen in the fitness profile across the three "continents" (Fig 2A). After steady outward fitness gradients are established at about t=250, genetic signatures migrate outwards, down the gradients. Signatures in the periphery are thus regularly overprinted by those coming from the centre.

Fig 2. Time evolution over 1000 steps of genome signatures along a profile x-y through the three continents. Map view of genetic variations is shown at stages 500 and 1000. Colours qualitatively represent variations in genome, with the red tones proportional to "fitness". Graphs show the fitness profiles for four time steps. **A.** In case of diffusion only, genetic signatures tend to emanate from the centre of the occupied areas and spread out towards the margins. **B.** When assortative mating is added, internally relative homogeneous "nation" regions with sharp boundaries develop from about t=500 steps. As these boundaries inhibit spreading of mutations, overall fitness increases more slowly than without assortative mating.

The effect of assortative mating

The effect of the assortative mating factor (α) is to reduce the rate of gene exchange when the genomes of neighbouring demes are different. Figure 2B shows the effect of assortative

mating in the same model as Fig 2A, but with α set to 0.05. This means decreasing genetic exchange up to ΔG=20, where exchange is reduced to zero. With initially low variations in genetic signature, the effect in the beginning is only to slow down differentiation. At about t=500, first neighbouring demes cease exchanging alleles, which allows their ΔG to increase further. This finally leads to homogeneous regions, bounded by fixed, sharp borders. In Fig. 2B these are visible as persistent, sharp changes in colour. New mutations cannot escape these "nations". Because the fixation time within a “nation” is smaller than for the whole model, these mutations can now spread significantly before more mutations occur, thus keeping ΔG and ΔF low within a "nation", while F for each "nation" keeps rising steadily. A large area, high mutation rate and low spreading rate (low D_0 and p) all favour high values of both ΔF and ΔG (with $\Delta G \geq \Delta F$). When these values remain too low, incipient borders shift and weaken again, which inhibits the establishment of permanent borders. This effect is visible in the medium and small "continents" that now behave as a closed system with highest fitness in the centre, but no internal "nation" borders. The development of "nations" or a structured population [66] results in a breakdown of the positive relationship (Fig 2A) between genetic signature and distance between points or isolation by distance [67]. This leads to a relative isolation of demes, which is strengthened through time.

Effect of replacement sweeps

The effect of replacement is again illustrated with the three-continent model (Fig 3), using the same p=0.05 and M of four mutations per time step as before. ΔF_{crit} is set at 10, so the

313 genome of a deme is fully replaced by that of its neighbour if that neighbour has at least 10
314 mutations more.
315
316 **Fig 3. Evolution of genetic signatures in case of replacement sweeps in the absence of**
317 **assortative mating. A.** Temporal evolution along the line x-y through the centre of the
318 model. Sharp changes in colour indicate replacement sweeps. The main ones are
319 highlighted in yellow. Graph shows the area (relative to total area) of individual sweeps as a
320 function of time. Replacement sweeps are strongly clustered in time. Map views show the
321 genetic distribution at selected points in time. Direction and extent of selected sweeps are
322 shown by yellow arrows and white lines that trace the front at regular intervals,
323 respectively. Doubling (**B**) or halving (**C**) the deme size roughly doubles or halves,
324 respectively, the average time interval between clusters of replacement sweeps, but not the
325 general pattern.
326
327 In the absence of assortative mating (α=0), fitness increases steadily, especially in
328 the centre of the model, until gradients exceeding ΔF_{crit} are reached (at t=274 in Fig 3A).
329 This typically happens somewhere between the centre and the margin. This is because,
330 although fitness is highest in the centre, gradients are generally low here. Gradients are
331 highest near the margins, where fitness is lower than in the centre. As a result,
332 replacements first sweep the margins of the model (t=274), skirting the high-fitness centre
333 (for example at t=296). Demes in the swept area with a single genome subsequently
334 exchange alleles with the unswept demes, which rapidly leads to genomes with enhanced
335 fitness again, and, hence, new sweeps (t=299). A rapid succession of admixture and

replacement sweeps leads to homogenisation of the genome over the whole area. Although the new global genome is closest to that of the centre of the model, there are significant changes by admixture during the various successive sweeps.

After homogenisation of the genome, it takes some time for gradients to develop again to initiate a new cycle of replacement sweeps. This leads to a regular cycle of 200-300 time steps of differentiation without any sweeps, followed by a rapid succession of many small and a few large sweeps that sweep almost the whole model area (Fig. 3A). This pattern is in line with the punctuated-equilibrium model [68-70]. Reducing the resolution by a factor two, while keeping all other parameters the same, implies reducing the population density and the frequency of mutations in the model by a factor four. Gradients now increase at a lower rate and the duration of a full cycle is roughly doubled (Fig 3B). Doubling the resolution has the opposite effect and leads to a reduction of the cycle time (Fig 3C). Independent of resolution, admixture results in several large sweeps that together reset the genomes in the whole area.

Adding assortative mating (α=0.05) to the previous simulation significantly changes the evolution of the model (Fig 4A). After the initial differentiation period, first sweeps occur and, again, mostly sweep the margins. Contrary to the previous case where α=0, the sweeping genome is now unlikely to interbreed with fit demes at the edge of the swept area owing to their large ΔG. New sweeps are thus not immediately triggered for lack of admixture, and sweeps are less clustered in time. Demes in the centre are rarely or even never swept, providing a genetic continuity here. These demes have a higher fitness than the surrounding homogenised swept areas, and thus have a higher chance to initiate future sweeps. Marginal areas show distinct extinction events, as can be seen by distinct colour

359 changes in Fig. 4B. Halving or doubling the resolution has the expected effect of increasing,
360 respectively decreasing the time between sweeps (Fig 4B-C).
361
362 **Fig 4. Evolution of genetic signatures in case of replacement sweeps as in Fig 3, but**
363 **now with additional assortative mating. A.** Temporal evolution along the line x-y
364 through the centre of the model. Sharp changes in colour indicate replacement sweeps. The
365 main ones are highlighted in yellow. Note the overall continuity in time of genomes in the
366 centre of the large continent that is rarely swept by migration waves. Graph shows the area
367 (relative to total area) of individual sweeps as a function of time. Replacement sweeps are
368 less clustered in time than in case of no assortative mating. Map views show the genetic
369 distribution at selected points in time. Direction and extent of selected sweeps are shown
370 by yellow arrows and white lines that trace the front at regular intervals, respectively.
371 Doubling (**B**) or halving (**C**) the deme size roughly doubles or halves, respectively, the
372 average time interval between clusters of replacement sweeps, but not the general pattern.
373
374 Figures 3 and 4 show that marginal areas, in particular the small continent
375 experience more sweeps than the centre of the area inside the large continent. The
376 simulations shown in Figs 3A and 4A were also run for 10,000 steps, recording each time a
377 deme was swept. Figure 5A shows that the chance for the two smaller continents and the
378 margins of the large continent to be swept is about 1.5 times higher than in for the centre of
379 the large continent in the absence of assortative mating. In case of assortative mating, the
380 effect is even stronger. Demes in the centre of the largest continent thus have a much higher
381 chance to be preserved, as these demes are rarely swept. This also affects the survival

382 chance of mutations. The origins of mutations that reached fixation are plotted in Fig. 5B.
383 We see that these are strongly concentrated in the centre of the large continent. While this
384 continent occupies 76% of the whole model area, it is the origin of >99% of all mutations
385 that reached fixation. The medium continent with 19% of the area delivered only <1% of all
386 mutations that reached fixation and the small continent not a single one. The chance of a
387 mutation from the medium continent to reach fixation is only 3.5% that of a mutation in the
388 large continent in the simulation without assortative mating. In the simulation with
389 assortative mating this change reduced to 1.7%. Replacement sweeps thus strongly favour
390 the survival of mutations from the centre of the largest populated landmass.

391 Directions of sweeps without (settings of Fig 3A) and with assortative mating
392 (settings of Fig 4A) were recorded for simulations running 10,000 steps. Mean sweep
393 propagation directions can be determined from this, and in turn, mean migration paths (Fig
394 5C). Migration paths consistently emanate from the centre of the large continent and lead to
395 its margin and to the smaller continents. Migration directions are more consistent in case of
396 assortative mating, resulting in a more consistent pattern of paths in the centre of the large
397 continent.

398

399 **Fig 5. Origin of fixed mutations, as well as distribution and directions of sweeps. A.**
400 Origin of mutations that reached fixation shown at black dots on the map. Mutations that
401 form in the middle of the large continent have a much larger chance of reaching fixation in
402 the whole model area than mutations deriving from the margins, especially the small
403 continent. **B.** Relative frequency that a deme is swept by a migration wave. Demes on the
404 margins and small continents are swept more often than demes in the centre of the large

405 continent. These patterns are more pronounced in case of assortative mating (below)
406 relative to the run without assortative mating. **C.** Average directions of migrations within
407 sweeps. Setting as in figures 3A (top) and 4A (bottom), run for 10,000 steps. C:
408
409 ## Fixation rate variation
410
411 After an initial period in which the system settles to a dynamic equilibrium, the number
412 (N_{fix}) of mutations that reach fixation (i.e. spreading over entire model area) increases
413 linearly with time (Fig 6). In the absence of replacement sweeps, N_{fix} increases steadily,
414 whereas the N_{fix}-time curve is stairway-like with replacement sweeps. This is because large
415 replacement sweeps spread some mutations over large areas, resulting in a sudden, but
416 temporary increase in fixation events. As the fitness landscape is flattened after these
417 events, few mutations can subsequently reach fixation until the process is repeated again.
418
419 **Fig 6. Number (N_{fix}) of mutations that reached fixation as a function of time with**
420 **linear regression lines (for t>600 steps).** Main graph shows the first 1000 time steps,
421 while the inset shows graphs for the full 5000 time steps on which the linear regressions
422 are based. Intersection of the linear regressions is the mean time to fixation (t_{fix}), while the
423 slope is the rate at which mutations reach fixation. Replacement sweeps reduce the fixation
424 chance of mutations by 60-70%, but also their t_{fix} by 3-5 times.
425
426 The time-averaged fixation chance (P_{fix}) of an individual mutation is derived from
427 the slope of the N_{fix}-time curve. P_{fix} is significantly lowered by replacement sweeps. With

interbreeding only, advantageous mutations are usually added to neighbouring genomes and few are lost by genetic drift before fixation, except at the nucleation phase just after the mutation occurred. Mutations in demes that are swept by replacement sweeps are lost, thus reducing the number of mutations that reach fixation [71]. Each wave causes a founder event, where only the limited genetic sample suddenly spreads over a large area [71-73]. The effect is more pronounced in case of assortative mating. The intersection of the linear regression of the N_{fix}-time curve with the horizontal time axis (Fig 6) gives the mean time to fixation (t_{fix}) for mutations that reach fixation. t_{fix} is about 4 times smaller in case of replacement sweeps than without these. This is to be expected, as replacement sweeps provide an efficient means to spread mutations over the map.

The reduced t_{fix} resulting from replacement sweeps has the advantage that a species can more quickly adapt to changes in the environment. This would cause some mutations to loose, and other to gain competitiveness. The latter can spread quickly in case of replacement sweeps. However, an inclination of a species towards replacements (low ΔF_{crit}) comes at a cost. Replacement sweeps imply that part of the population is excluded and inhibited from further contributing to the species through their offspring. Furthermore, our simulations that are intentionally without any environmental changes show that a low ΔF_{crit} also leads to spontaneous replacement sweeps in the complete absence of any external factors.

Sweep area statistics

Although the largest sweeps are the most conspicuous in Figs 3 and 4, these are accompanied by many more smaller sweeps. Figure 7 shows the frequency (f) of sweep areas versus their normalised area (A_n = sweep area/model area). We see that that the data plot on a straight line in the double-log plot, indicating a power-law relationship between f and A_n, with an exponent -q:

$$f \propto (A_n)^{-q}, \quad (8)$$

at least when A_n is small (up to a few per cent of the total area). A power law (Eq. 8) was fitted to the data for A_n<0.01 from simulations shown in Figs. 3 and 4, but run for up to 10,000 steps, resulting in q-values ranging from 1.81 to 2.09. Frequencies were normalised such that the power-law best fit frequency for A_n=1 is unity in each of the six simulations. All these normalised data together overlap remarkably well (Fig 7). We obtain q=1.84 when applying a best fit to all data with A_n<0.01. Normalised sweep areas >0.02 are overrepresented, with their frequencies up to >10x higher than the power-law trend. Notwithstanding this, small sweeps are orders of magnitude more common than the largest ones.

Fig 7. Normalised frequency distribution of areas swept by migration waves plotted against these areas (divided by total area) in a double-log plot. Data follow a power-law, except for the very largest sweeps. Dots represent the simulations with the schematic 3-continent map shown in figs. 3 and 4, but with 10,000 time steps.

The observed power-law relation is a hallmark of the self-organised criticality (SOC) model of Bak et al. [74] that has been used [75, 70] to explain punctuated equilibria [69].

473 The classical SOC model is the (numerical) sand pile in which grains are randomly sprinkled
474 on a stage. Once critical heights of grain piles, or gradients in these heights are reached,
475 grains are redistributed locally. One redistribution event can lead to neighbouring sites
476 reaching the criterion for redistribution, sometimes leading to large "avalanches". Sizes of
477 these avalanches typically follow power-law distributions, as the critical state has no
478 intrinsic time or length scale [74]. The current model is similar to the classical sand-pile
479 model, as mutations are "sprinkled" on the map of demes. There is a criterion for
480 redistribution (ΔF_{crit}), which leads to replacement sweeps that indeed follow a power-law
481 frequency distribution (Fig. 8). A first difference with the standard sand-pile model is that,
482 contrarily to grains, mutations can multiply. The second is that the model includes diffusion
483 as an additional transport mechanism for mutations. Models with two transport channels,
484 one fast avalanche-like and one diffusional, have been applied to fluid flow through pores
485 and fractures [76, 77], earthquake evolution [78, 79], and heat transport in plasmas [80].
486 These models show that such systems still exhibit SOC-characteristics, as long as the
487 criterion for the fast transport is frequently reached. However, with increasing importance
488 of diffusion, avalanches become more regularly spaced in time and larger, isolated events
489 (so-called "dragon kings" [81, 82]) become more common [80]. This behaviour is indeed
490 observed in our "mutation-pile" model, where large sweeps are over-represented
491 compared to small ones and there is strong (α=0) and weak (α=0.05) cyclical behaviour
492 with periods of semi-stasis (gradual diffusional differentiation), alternating with short
493 periods of replacement sweeps. As such the model shows punctuated-equilibrium
494 behaviour.
495

Application to a world map

Having assessed the effects of, and patterns resulting from the different parameters on a schematic map with three continents, we now briefly illustrate the potential implication for human evolution. For this purpose we used a Fuller-projection map of the Old World (Fig 8), roughly adapted to ice age conditions by linking Japan and the British Isles to the mainland and assuming that large parts of northern Europe and Asia are (effectively) not inhabited. Although population densities (ρ) would never have been equal throughout the inhabited area, we maintain the assumption of a constant ρ, but excluded high-elevation areas (especially Tibet and the Pamirs) and desert areas in North Africa and the Arabian Peninsula, adapted from Eriksson et al. [38] for ~21 ka BP. In this configuration inhabited areas in Africa occupy 44% of the whole inhabited area. Inhabited areas evidently varied over time, but this simplified model serves the purpose of predicting the main expected patterns. Deme size was set at 50x50 km, resulting in 20808 populated demes, and settings were equal to those for the simulations shown in figures 3A and 4A. At a time step of about 4000 years (for ρ=0.01 individuals/km^2), p=0.05 would lead to a mutation spreading rate of 0.002 km/yr (Eq. 5). Replacement sweeps in the current model take place within one time step. The maximum distance to travel, from South Africa to Japan is about 17,500 km, resulting in a maximum sweep velocity of ~4 km/yr. Such high velocities, however, only apply to the few very largest sweeps.

Fig 8. Example of applying the model for 10,000 steps with settings as in figures 3A and 4A to a map of the Old World. Top row without (α=0) and bottom row with

519 assortative mating (α=0.05). **A.** Mean fitness of demes over the whole simulation, showing
520 that demes in Central Africa are, on average, fitter than the minimum at the margins of the
521 populated area. **B.** Origin of all mutations that reached fixation. Most (α =0) or all (α =0.05)
522 these mutations originated in Africa. **C.** Number of times that a deme has been swept by a
523 migration wave. Demes in Central Africa experienced significantly fewer sweeps than the
524 rest of the world, especially in case of α=0.05. **D.** Mean migration paths, all emanating from
525 central Africa and diverging towards the periphery of the continent and into Asia.
526
527 In both simulations, with and without assortative mating, mean fitness is highest in central
528 Africa (Fig 8A). The fitness maximum is most distinct in case of α=0, because the long and
529 regular interval between clusters of sweep events allow large-scale gradients to develop.
530 Mutations that reach fixation mostly come from central Africa (Fig 8B). When α=0.05 no
531 mutations that originated outside of Africa reach fixation. When α=0, a few mutations from
532 Asia reach fixation, because sweeps from Africa can trigger "counter" sweeps after
533 admixture with genomes from the margin of the swept areas. The chance that a deme in
534 central Africa is swept by a migration event is higher in case of α=0 than when α=0.05 (Fig
535 8C). Despite these differences, migration directions are mostly emanating from central
536 Africa in the direction of the margins of the occupied area (Fig 8D).
537 Sweep area frequencies follow the same power-law distribution (Eq. 8, Fig 9A) as in
538 the abstract 3-continent model. Largest sweeps are again over-represented relative to the
539 power-law trend for smaller sweeps. The effect becomes noticeable for sweeps that are
540 larger than a few per cent of the total area. This is about 1/3 the area of Europe. The
541 frequency distributions show two distinct peaks. One is at the area of Japan, which in the

542 model forms a narrow peninsula connected to Asia. Sweeps apparently initiate at the
543 connection with the peninsula (where mutations rarely occur) and then tend to sweep the
544 whole peninsula. The second peak is at about 56% of the total area, which equals the area of
545 Eurasia. This indicates that isthmuses, such as the Sinai Peninsula, play an important role
546 and sweeps from Africa that entered Asia have an increased chance of then sweeping the
547 whole of Eurasia.
548
549 **Fig 9. Sweep statistics of simulations for the Old World. A.** Graph of normalised
550 frequency as a function of sweep area. **B.** Cumulative graph of number of sweeps against
551 sweep area. About 1% of all sweeps are the size of Eurasia (56% of total area) or larger. **C.**
552 Cumulative graph of the areas swept as a function of sweep area. About 50% of all
553 individual deme replacements result from sweeps are the size of Eurasia (56% of total
554 area) or larger.
555
556 The cumulative number of sweeps as a function of area (Fig 9B) shows that sweeps
557 of the size of Eurasia or larger represent about 1% of all sweeps. However, these few
558 sweeps are responsible for about 50% of all individual deme replacement events over time
559 (Fig 9C). If in the past there were one or two major out-of-Africa sweeps, one can deduce
560 that there were in the order of 100-200 replacement sweeps in total. The average number
561 of sweeps that an individual population in one single deme would have experienced would
562 be about 2-4, double the number of very large sweeps. Two to four replacement events in a
563 million years, i.e. ~40,000 generations, means that individuals in a deme have a chance in
564 the order of 0.005-0.01% of experiencing a replacement sweep in their lifetime. Although

565 sweeps thus rarely affect individuals, they have a profound effect on the evolution of the
566 human genome, because about half these locally experienced sweeps are part global-scale
567 sweeps that span a significant part of the whole populated Old World.
568

569 # Conclusions

570 Diffusional gene flow alone leads to a homogenisation of all populations [83]. However,
571 ongoing mutations continuously produce local variations that take time to spread over the
572 whole populated area. The combination of diffusion and mutations thus results in isolation
573 by distance [67], with differences between local populations increasing with distance (Fig.
574 2A). The magnitude of these differences or clines depends on the balance between diffusion
575 and mutation rate. The effect of assortative mating is to create a structured population [66]
576 with relatively homogeneous "nation" regions, separated by distinct clines. While Scerri et
577 al.[66] argue that the structuring is due to environmental and ecological drivers, our model
578 (Fig 2B) shows that structuring can develop due to assortative mating without any such
579 additional drivers. Without other evolutionary mechanisms, assortative mating reduces or
580 inhibits exchange between regions and this exchange is restricted to neighbouring regions.
581 Migration events are an efficient way to bring populations from far-removed regions into
582 contact. Ensuing exchange across such new contacts leads to reticulate phylogenies [63].

583 Our model shows that, if population/species replacements do occur, replacement
584 sweeps of all sizes up to the whole populated area are expected. The basic reason is that if
585 one group of individuals can take over the area of their neighbours, the chance that they (or
586 their offspring) can also take over the next area is larger than zero. This can, but must not,
587 lead to "avalanches" of replacements that can span up to the whole populated area.

588 Replacement-sweep-area frequencies systematically decrease as a power-law function of
589 their area. For every world-spanning sweep, about two orders of magnitude smaller sweeps
590 are to be expected, down to the size of one deme in the model. As expected, isthmuses
591 appear to play a special "bottle neck" role during expansions. Once a sweep crosses an
592 isthmus, there is an increased chance that the whole peninsula beyond is swept in its
593 entirety. In simulations this leads to a distinct peak in the chance that the whole of Eurasia
594 is swept in at an out-of-Africa event.

595 Replacement sweeps reduce the chance of fixation of mutations, but also
596 significantly reduce the time to fixation of those mutations that do finally reach fixation. The
597 propensity of a population to usurp the area of its neighbours if these are, for some reason,
598 less competitive, has the benefit that advantageous mutations can quickly spread, for
599 example after a change in environmental conditions. However, our simulations show that
600 this propensity inevitably also leads to spontaneous replacement sweeps that are not
601 triggered by any external factors but driven by genetic drift.

602 Our simulations show that replacement sweeps mostly emanate from the largest
603 consolidated populated area. In the Old World this is Africa, especially during glaciation
604 stages. The simulations indicate that the most likely origin for modern humans lies
605 somewhere in (central) Africa, in line with what is deduced from the fossil record (e.g. [84]).
606 However, East Asia also forms large and compact populated area, especially during warm
607 periods, that would have been a second probable source for replacement sweeps. This
608 emphasizes the need for further palaeoanthropological research in East Asia (e.g. [85, 5]).

609 Large migration sweeps generally emanate from the central regions of large compact
610 areas and spread towards the margins. The spreading directions are mostly determined by

611 coastlines, mountains and other uninhabited areas. This leads to a remarkable consistency
612 of the directions, quite independent of the parameter settings (Fig 8C). The tendency to
613 migrate towards coasts is consistent with the beachcomber model [86]. The spreading of a
614 migration wave is more like that of an inkblot than along narrow, bifurcating migration
615 paths that some authors envisage [87].

616 Mutations that arise in the centre of large compact areas have the highest change to
617 survive and spread. This is not only because these areas are the probably sources of
618 migration sweeps, but they are also the least likely to be swept themselves (Fig 8C). This
619 pattern illustrates the relevance of the central areas as potential sources of new variants,
620 but also in preserving old traits.

621 Considering a combination of semi-stasis periods alternating with replacement
622 sweeps as a result of large-scale and many smaller expansions may contribute to
623 understand the current biological distribution of human populations, as well as the
624 variation in the hominin fossil record. For this reason we suggest an integration of concepts
625 coming from punctuated equilibrium theory [68,70,75], multiregional postulates [24, 62, 63,
626 66], and current out-of-Africa migration models. Any migration wave that spanned the
627 whole world is most likely to have come from Africa. If large migration waves can occur,
628 more numerous smaller waves are to be expected too. Multiple out-of-Africa waves are,
629 therefore, most likely if one happened. Although the propensity for replacement waves
630 makes a species more adaptable to changes in its environment, a "side effect" is that such
631 waves then also occur spontaneously. A spontaneous emergence and spread of modern
632 humans from Africa should thus be regarded as a null hypothesis against which any
633 hypothetical causes should be tested.

References

1. Tattersall I. Paleoanthropology: the last half-century. Evol Anthropol. 2000; 9: 2–16.
2. Foley R. In the shadow of the modern synthesis? Alternative perspectives on the last fifty years of paleoanthropology. Evol Anthropol. 2001; 10: 5–14.
3. Bräuer G. The origin of modern anatomy: by speciation or intraspecific evolution? Evol Anthropol. 2008; 17: 22–37.
4. Dennell RW. The colonization of "Savannahstan": issues of timing(s) and patterns of dispersal across Asia in the Late Pliocene and Early Pleistocene. In: Asian Paleoanthropology. Springer, Dordrecht; 2011. 7-30.
5. Zhu Z, Dennell R, Huang W, Wu Y, Qiu S, Yang S, et al. Hominin occupation of the Chinese Loess Plateau since about 2.1 million years ago. Nature. 2018; doi: 10.1038/s41586-018-0299-4.
6. White TD, Asfaw B, DeGusta D, Gilbert H, Richards GD, Suwa G, et al. Pleistocene *Homo sapiens* from Middle Awash, Ethiopia. Nature. 2003; 423: 742–747.
7. McDougall I, Brown FH, Fleagle JG. Stratigraphic placement and age of modern humans from Kibish, Ethiopia. Nature. 2005; 433: 733–736.
8. Hublin, JJ, Ben-Ncer A, Bailey SE, Freidline SE, Neubauer S, Skinner MM, et al. New fossils from Jebel Irhoud, Morocco and the pan-African origin of *Homo sapiens*. Nature. 2017; 546: 289-292. doi: 10.1038/nature22336.
9. Lahr MM, Foley R. Multiple dispersals and modern human origins. Evol Anthropol. 1994; 3: 48–60.

656 10. Conard NJ, Bolus M. Radiocarbon dating the appearance of modern humans and
657 timing of cultural innovations in Europe: new results and new challenges. J Hum Evol.
658 2003; 44: 331-371.
659 11. Hershkovitz I, Weber GW, Quam R, Duval M, Grün R, Kinsley L, et al. The earliest
660 modern humans outside Africa. Science. 2018; 359: 456-459.
661 12. Mellars P, French, CJ. Tenfold Population Increase in Western Europe at the
662 Neandertal–to–Modern Human Transition. Science. 2011; 333: 623-627.
663 13. Groucutt HS, Petraglia MD, Bailey G, Scerri EM, Parton A, Clark‐Balzan L, et al.
664 Rethinking the dispersal of Homo sapiens out of Africa. Evol Anthropol: Issues, News,
665 and Reviews. 2015; 24(4): 149-164.
666 14. Krings M, Stone A, Schmitz RW, Krainitzki H, Stoneking M, Pääbo S. Neanderthal DNA
667 sequences and the origin of modern humans. Cell. 1997; 90(1): 19-30.
668 15. Krings M, Geisert H, Schmitz RW, Krainitzki H, Pääbo S. DNA sequence of the
669 mitochondrial hypervariable region II from the Neanderthal type specimen. Proc Natl
670 Acad Sci U S A. 1999; 96: 5581-5585.
671 16. Krings M, Capelli C, Tschentscher F, Geisert H, Meyer S, Haeseler A. A view of
672 Neanderthal genetic diversity. Nat Genet. 2000; 26: 144-146.
673 17. Brown P, Sutikna T, Morwood MJ, Soejono RP, Jatmiko E, Wayhu Saptomo E., et al. A
674 new small-bodied hominin from the Late Pleistocene of Flores, Indonesia. Nature.
675 2004; 431: 1055–1061.
676 18. Morwood MJ, Soejono RP, Roberts RG, Sutikna T, Turney CSM, Westaway KE, et al.
677 Archaeology and age of a new hominin from Flores in eastern Indonesia. Nature.
678 2004; 431: 1087–1091.

679 19. Morwood MJ, Brown P, Sutikna T, Saptomo EW, Westaway KE, Due RA, et al. Further
680 evidence for small-bodied hominins from the Late Pleistocene of Flores, Indonesia.
681 Nature. 2005; 437: 1012–1017.
682 20. Krause J, Orlando L, Serre D, Viola B, Prüfer K, Richards MP, et al. Neanderthals in
683 central Asia and Siberia. Nature. 2007; 449: 902-904.
684 21. Krause J, Fu Q, Good JM, Viola B, Shunkov MV, Derevianko AP, et al. The complete
685 mitochondrial DNA genome of an unkown hominin from southern Siberia. Nature.
686 2010; 464: 894-897.
687 22. Higham T, Douka K, Wood R, Ramsey CB, Brock F, Basell L, et al. The timing and
688 spatiotemporal patterning of Neanderthal disappearance. Nature. 2014; 512: 306-309.
689 Doi: doi:10.1038/nature13621.
690 23. Posth C, Wißing C, Kitagawa K, Pagani L, van Holstein L, Racimo F, et al. Deeply
691 divergent archaic mitochondrial genome provides lower time boundary for African
692 gene flow into Neanderthals. Nat Commun. 2017; 8: 16046.
693 24. Cavalli-Sforza LL, Menozi P, Piazza A. Demic expansions and human evolution. Science.
694 1993; 259: 639-646.
695 25. Hublin JJ. The modern human colonization of western Eurasia: when and where? Quat
696 Sci Rev. 2015; 118: 194-210.
697 26. Nigst PR, Haesaerts P, Damblon F, Frank-Fellner C, Mallol C, Viola B, et al. Early
698 modern human settlement of Europe north of the Alps occurred 43,500 years ago in a
699 cold steppe-type environment. PloS ONE. 2014; 111: 14394-14399.
700 27. Reed FA, Tishkoff SA. African human diversity, origins and migrations. Curr Opin
701 Genet Dev. 2006; 16: 597–605.

28. Skoglund P, Thompson JC, Prendergast, ME. Reconstructing Prehistoric African Population Structure. Cell. 2017; 171: 59–71.

29. Fu Q, Posth C, Hajdinjak M, Petr M, Mallick S, Fernandes D, et al. The genetic history of Ice Age Europe. Nature. 2016; 534: 200-205.

30. Posth C, Renaud G, Mittnik A, Drucker DG, Rougier H, Cupillard C, et al. Pleistocene Mitochondrial Genomes Suggest a Single Major Dispersal of Non-Africans and a Late Glacial Population Turnover in Europe. Curr Biol. 2016; 26: 827-833.

31. Banks WE, d'Errico F, Peterson AT, Kageyama M, Sima A, Sanchez-Goni MF. Neanderthal extinction by competitive exclusion. PloS ONE. 2008; 3(12): e3972.

32. Agustí J, Rubio-Campillo X. Were Neanderthals responsible for their own extinction? Quat Int. 2017; 431: 232-237.

33. Gilpin W, Feldman MW, Aoki K. An ecocultural model predicts Neanderthal extinction through competition with modern humans. Proc Natl Acad Sci U S A. 2016; 113(8): 2134-2139.

34. d'Errico F, Sánchez Goñi MF. Neandertal extinction and the millennial scale climatic variability of OIS 3. Quat Sci Rev. 2003; 22: 769-788.

35. Tzedakis PC, Hughen KA, Cacho I, Harvati K. Placing late Neanderthals in a climatic context. Nature. 2007; 449: 206-208.

36. Müller UC, Pross J, Tzedakis PC, Gamble C, Kotthoff U, Schmiedl G, et al. The role of climate in the spread of modern humans into Europe. Quat Sci Rev. 2011; 30: 273-279.

37. Rosenberg TM, Preusser F, Fleitmann D, Schwalb A, Penkman K, Schmid TW, Al-Shanti MA, Kadi K, Matter A. Humid periods in southern Arabia: Windows of opportunity for modern human dispersal. Geology. 2011; 39: 1115-1118.

725 38. Eriksson A, Betti L, Friend AD, Lycett SJ, Singarayer JS, von Cramon-Taubadel N,
726 Valdes PJ, Balloux F, Manica A. Late Pleistocene climate change and the global
727 expansion of anatomically modern humans. Proc Natl Acad Sci U S A. 2012; 109:
728 16089–16094.
729 39. Grove M, Lamb H, Roberts H, Davies S, Marshall M, Bates R, et al. Climatic variability,
730 plasticity, and dispersal: A case study from Lake Tana, Ethiopia. J Hum Evol. 2015; 87:
731 32-47.
732 40. Maslin MA, Shultz S, Trauth MH. A synthesis of the theories and concepts of early
733 human evolution. Phil Trans R Soc B. 2015; 370: 20140064.
734 http://dx.doi.org/10.1098/rstb.2014.0064
735 41. Timmermann A, Friedrich T. Late Pleistocene climate drivers of early human
736 migration. Nature. 2016; 538, 92-95.
737 42. Lamb HF, Bates CR, Bryant CL, Davies SJ, Huws DG, Marshall MH, et al. 150,000-year
738 palaeoclimate record from northern Ethiopia supports early, multiple dispersals of
739 modern humans from Africa. Sci Rep. 2018; 8(1): 1077.
740 43. Kolodny O, Feldman MW. A parsimonious neutral model suggests Neanderthal
741 replacement was determined by migration and random species drift. Nat Commun.
742 2017; 8(1): 1040.
743 44. Bocquet-Appel JP, Demars PY. Population Kinetics in the Upper Palaeolithic in
744 Western Europe. J Archaeol Sci. 2000; 27: 551-570, doi:10.1006/jasc.1999.0471
745 45. Bocquet-Appel JP, Demars PY, Noiret L. Dobrowsky D. Estimates of Upper Palaeolithic
746 meta-population size in Europe from archaeological data. Journal of Archaeological
747 Science. 2005; 32: 1656-1668, doi:10.1016/j.jas.2005.05.006

748 46. Bocquet-Appel JP, Degioanni A. Neanderthal Demographic Estimates. Curr Anthropol.
749 2013; 54: S202-S213, doi:10.1086/673725
750 47. Blum MGB, Jakobsson M. Deep Divergences of Human Gene Trees and Models of
751 Human Origins. Mol Biol Evol. 2011; 28; 889–898, doi 10.1093/molbev/msq265.
752 48. Hoban S, Bertorelle G, Gaggiotti OE. Computer simulations: tools for population and
753 evolutionary genetics. Nat Rev. 2012; 13: 110-122. doi:10.1038/nrg3130.
754 49. Liu H, Prugnolle F, Manica A, Balloux F. A geographically explicit genetic model of
755 worldwide human-settlement history. Am J Hum Genet. 2006; 79: 230–237.
756 50. Ray N, Currat M, Foll M, Excoffier L. SPLATCHE2: A spatially explicit simulation
757 framework for complex demography, genetic admixture and recombination.
758 Bioinformatics. 2010; 26: 2993–2994.
759 51. Barton CM, Riel-Salvatore J. Agents of change: modeling biocultural evolution in Upper
760 Pleistocene western Eurasia. Adv Complex Syst. 2012; 15: 1150003, doi:
761 10.1142/S0219525911003359.
762 52. Benguigui M, Arenas M. Spatial and Temporal Simulation of Human Evolution.
763 Methods, Frameworks and Applications. Curr Genomics. 2014; 15: 245-255.
764 53. Rikvold PA, Zia RKP. Punctuated equilibria and 1/f noise in a biological coevolution
765 model with individual-based dynamics. Phys Rev E. 2003; 68: 031913, Doi:
766 10.1103/PhysRevE.68.031913.
767 54. Whitlock MC. Fixation Probability and Time in Subdivided Populations. Genetics.
768 2003; 164: 767–779.
769 55. Fisher RA. The Genetical Theory of Natural Selection. Oxford: Oxford University Press;
770 1930.

771 56. Fisher RA. The wave of advance of advantageous genes. Ann Eugen. 1937; 7: 355-369.
772 doi: 10.1111/j.1469-1809.1937.tb02153.x.
773 57. Kimura O, Ohta T. The average number of generations until fixation of a mutant gene
774 in a finite population. Genetics. 1969; 61: 763-771.
775 58. Gavrilets S. Perspective: Models of speciation: what have we learned in 40 years?
776 Evolution. 2013; 57: 2197-2215.
777 59. Haldane JBS. A mathematical theory of natural and artificial selection. V Proc Camb
778 Philos Soc. 1927; 23:838 – 844.
779 60. Wright S. Evolution in Mendelian populations. Genetics. 1931; 16: 97-159.
780 61. Lande R. Natural selection and random genetic drift in phenotypic evolution.
781 Evolution. 1976; 30: 314-334.
782 62. Wolpoff MH, Hawks J, Caspari R. Multiregional, Not Multiple Origins. Am J Phys
783 Anthropol. 2000; 112: 129-136
784 63. Winder IC, Winder NP. Reticulate evolution and the human past: an anthropological
785 perspective. Ann Hum Biol. 2014; 41: 300–311, doi: 10.3109/03014460.2014.922613
786 64. Bae CJ, Douka K, Petraglia MD. Human Colonization of Asia in the Late Pleistocene –
787 An introduction to Supplement 17. Curr Anthropol. 2017; 58(17): S373 – S382.
788 65. Galway-Witham J, Stringer C. How did Homo sapiens evolve? Science. 2018; 360:
789 1296-1298
790 66. Scerri EML, Thomas MG, Manica A, Gunz P, Stock JT, Stringer C. Did Our Species Evolve
791 in Subdivided Populations across Africa, and Why Does It Matter? Trends Ecol Evol.
792 2018; Doi: 10.1016/j.tree.2018.05.005.

793 67. Shennan SJ, Crema ER, Kerig T. Isolation-by-distance, homophily and 'core' vs.
794 'package' cultural evolution models in Neolithic Europe. Evol Hum Behav. 2015; 36:
795 103–109
796 68. Gould SJ, Eldredge N. Punctuated equilibria: the tempo and mode of evolution
797 reconsidered. Paleobiology. 1977; 3: 115-151;
798 69. Gould SJ, Eldredge N. Punctuated equilibrium comes of age. Nature. 1993; 366: 223-
799 227
800 70. Bak P, Boettcher S. Self-organized criticality and punctuated equilibria. Physica D.
801 1997; 107: 143-150.
802 71. Excoffier L, Foll M, Petit RJ. Genetic Consequences of Range Expansions. Annu Rev Ecol
803 Evol Syst. 2009; 40: 481–501.
804 72. Ramachandran S, Deshpande O, Roseman CC, Rosenberg NA, Feldman MW, Cavalli-
805 Sforza LL. Support from the relationship of genetic and geographic distance in human
806 populations for a serial founder effect originating in Africa. Proc Natl Acad Sci. 2005;
807 102:15942–15947.
808 73. Sugden LA, Ramachandran S. Integrating the signatures of demic expansion and
809 archaic introgression in studies of human population genomics. Curr Opin Genet Dev.
810 2016; 41:140–149
811 74. Bak P, Tang C, Wiesenfeld K. Self-organized criticality, Phys Rev A. 1988; 38: 364–374.
812 75. Bak P, Sneppen K. Punctuated Equilibrium and Criticality in a Simple Model of
813 Evolution. Phys Rev Lett. 1993; 71: 4083-4086.
814 76. Miller SA, Nur A. Permeability as a toggle switch in fluid-controlled crustal
815 processes. Earth Planet Sci Lett. 2000; 183(1-2): 133-146.

816 77. Bons PD, van Milligen BP. A new experiment to model self-organized critical transport
817 and accumulation of melt and hydrocarbons from their source rocks. Geology. 2001;
818 29: 919-922, doi: 10.1130/0091-7613
819 78. Sornette A, Sornette D. Self-organized criticality and earthquakes. Europhys Lett.
820 1989; 9(3): 197.
821 79. Olami Z, Feder HJS, Christensen K. Self-organized criticality in a continuous,
822 nonconservative cellular automaton modeling earthquakes. Phys Rev Lett.
823 1992; 68(8): 1244.
824 80. Sánchez R, Newman DE, Carreras BA. Mixed SOC diffusive dynamics as a paradigm for
825 transport in fusion devices. Nuclear Fusion. 2001; 41: 247-256.
826 81. Sachs MK, Yoder MR, Turcotte DL, Rundle JB, Malamud BD. Black swans, power laws,
827 and dragon-kings: Earthquakes, volcanic eruptions, landslides, wildfires, floods, and
828 SOC models. Eur Phys J Spec Top. 2012; 205: 167-182.
829 82. Sornette D, Ouillon G. Dragon-kings: mechanisms, statistical methods and empirical
830 evidence. Eur Phys J Spec Top. 2012; 205(1): 1–26.
831 83. Freeman S, Herron JC. Evolutionary analysis. New Jersey: Prentice Hall; 2004.
832 84. Stringer C. The origin and evolution of *Homo sapiens*. Phil Trans B. 2016; 371:
833 20150237.
834 85. Qiu J. The forgotten continent. Nature. 2016; 535:218-220.
835 86. Oppenheimer S. The great arc of dispersal of modern humans: Africa to Australia. Quat
836 Int. 2009; 202: 2–13.

837 87. Reyes-Centeno H, Ghirotto S, Détroit F, Grimaud-Hervé D, Barbujani G, Harvati K.
838 Genomic and cranial phenotype data support multiple modern human dispersals from
839 Africa and a southern route into Asia. Proc Natl Acad Sci U S A. 2014; 111: 7248-7253.

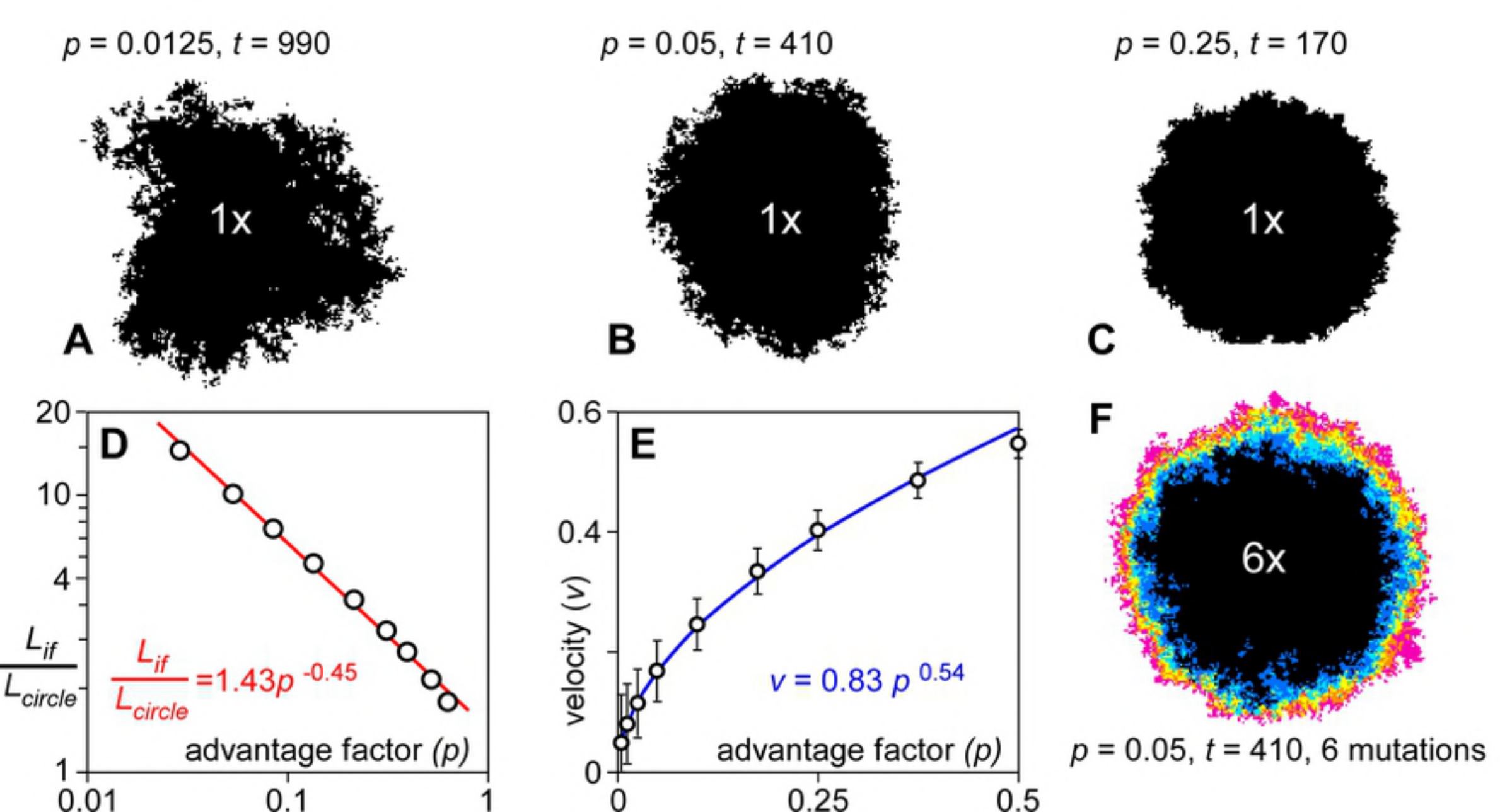
p = 0.0125, t = 990
p = 0.05, t = 410
p = 0.25, t = 170
1x
1x
1x
A
B
C
D
E
F
6x
20
10
4
1
0.01
0.1
1
L_if / L_circle
L_if / L_circle =1.43p -0.45
advantage factor (p)
0.6
0.4
0
0
0.25
0.5
velocity (v)
v = 0.83 p 0.54
advantage factor (p)
p = 0.05, t = 410, 6 mutations

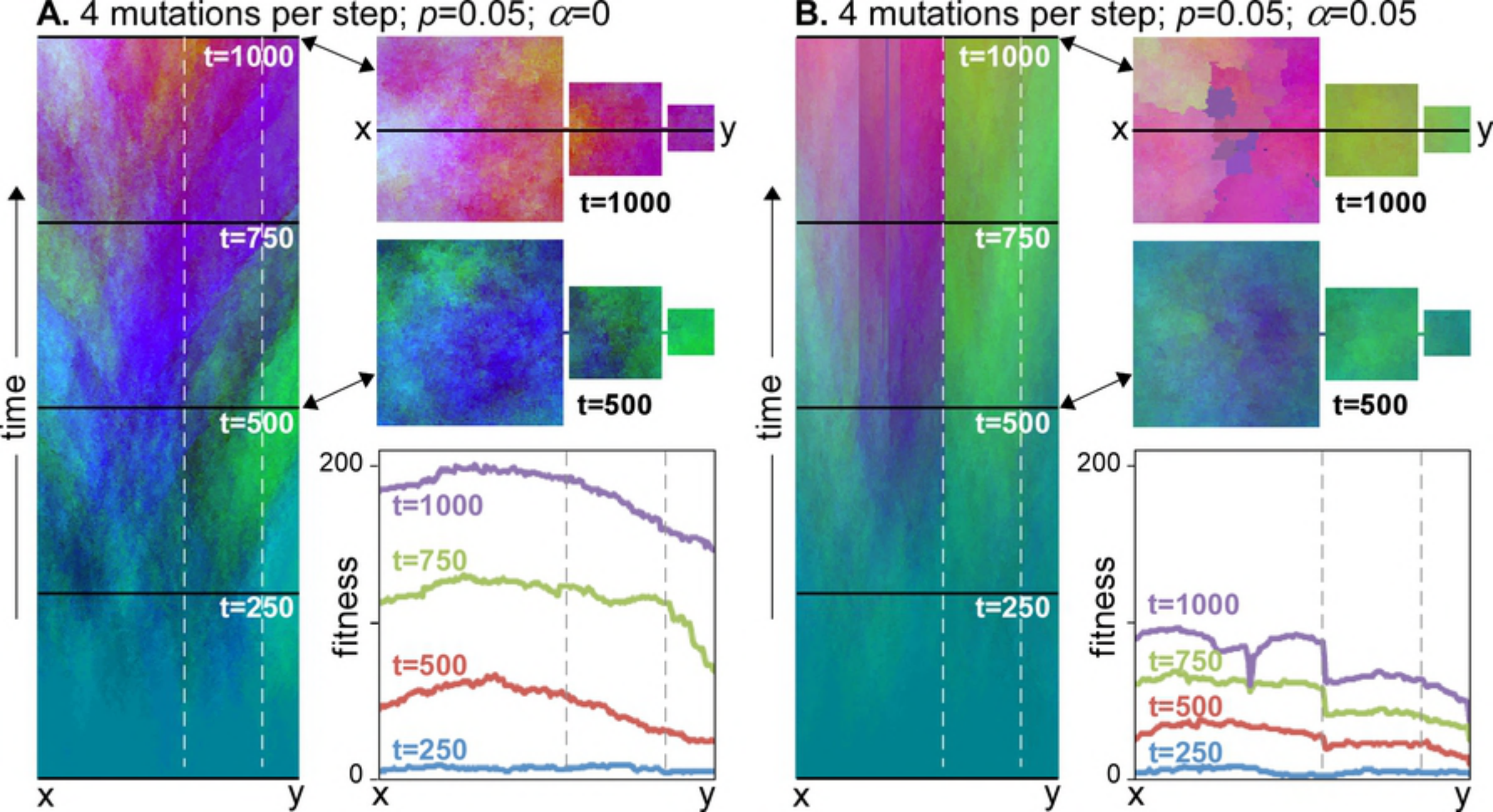
A. 4 mutations per step; p=0.05; α=0
B. 4 mutations per step; p=0.05; α=0.05
t=1000
t=750
t=500
t=250
time
x
y
fitness
200
0
t=1000
t=500

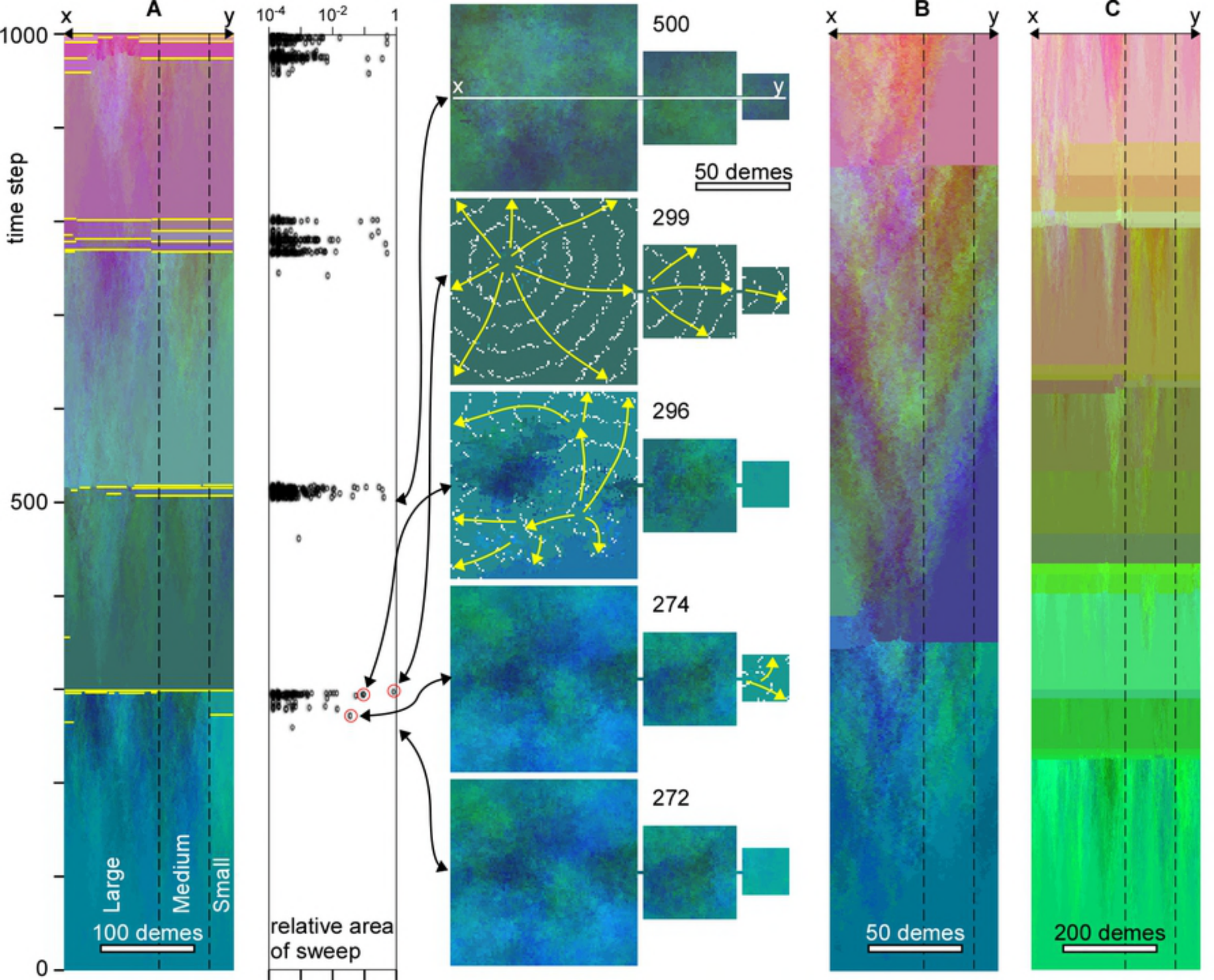
A
x
y
1000
500
0
time step
Large
Medium
Small
100 demes
10^{-4}
10^{-2}
1
relative area
of sweep
500
299
296
274
272
50 demes
B
50 demes
C
200 demes

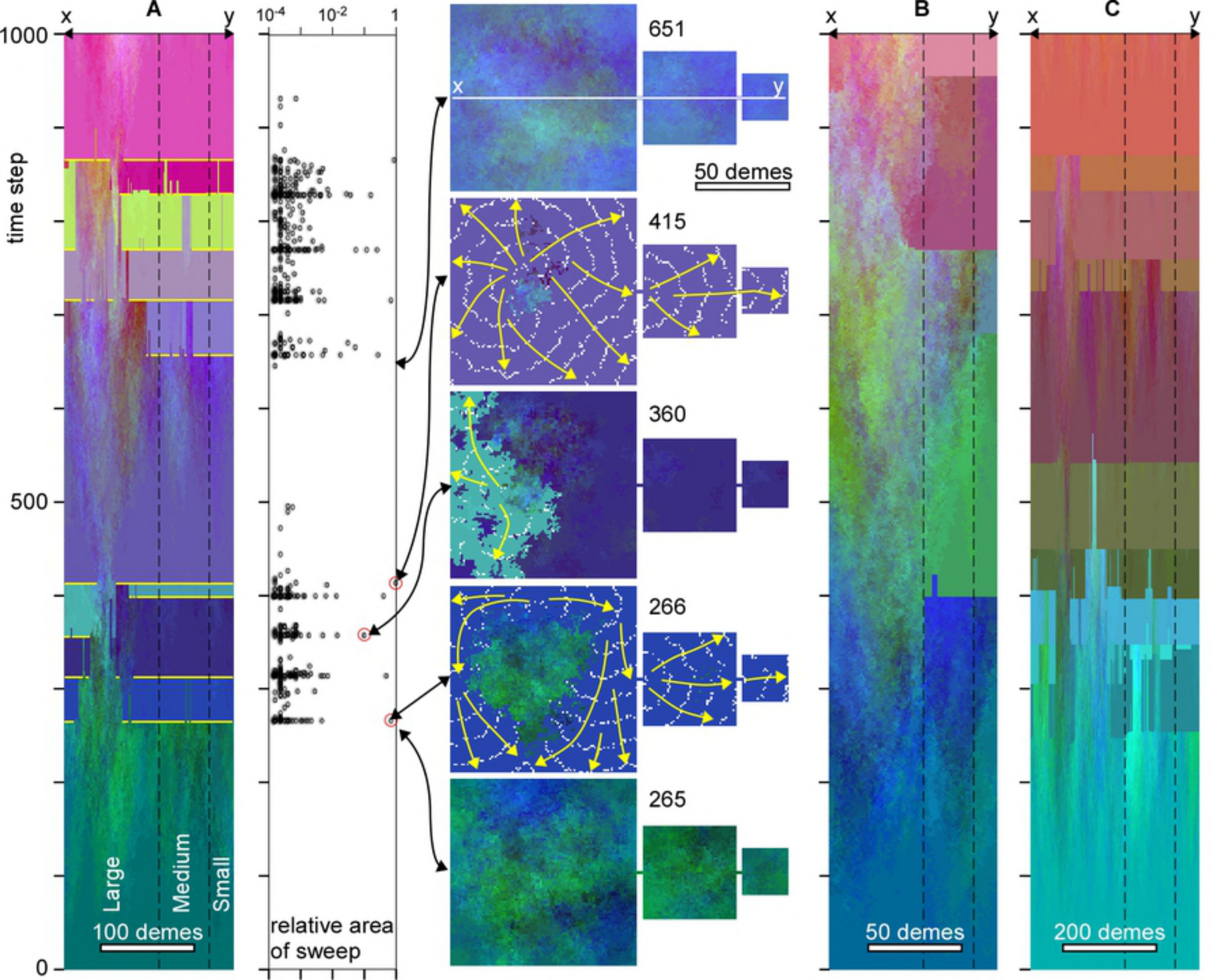
A
x
y
1000
500
0
time step
Large
Medium
Small
100 demes
10^{-4}
10^{-2}
1
relative area
of sweep
651
415
360
266
265
50 demes
B
50 demes
C
200 demes

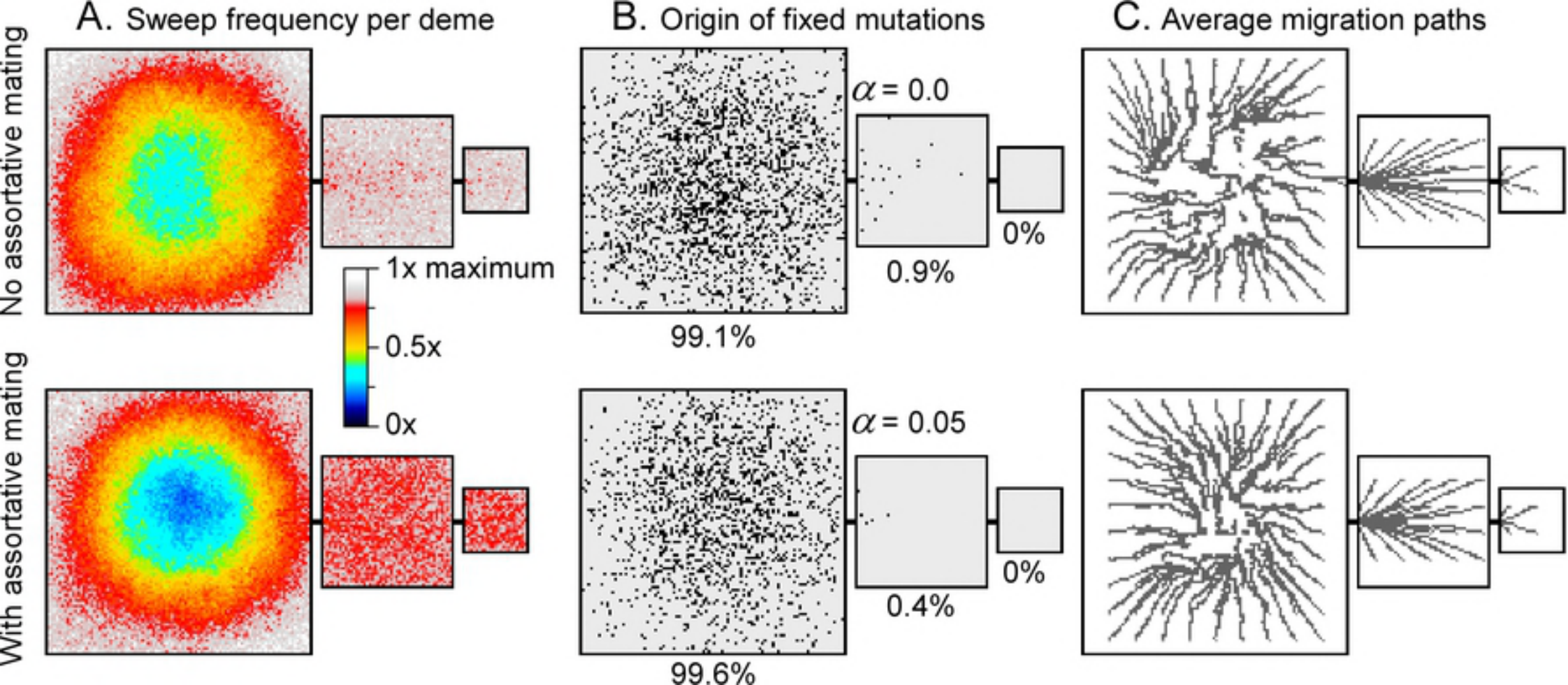
A. Sweep frequency per deme
B. Origin of fixed mutations
C. Average migration paths
No assortative mating
With assortative mating
1x maximum
0.5x
0x
α = 0.0
99.1%
0.9%
0%
α = 0.05
99.6%
0.4%
0%

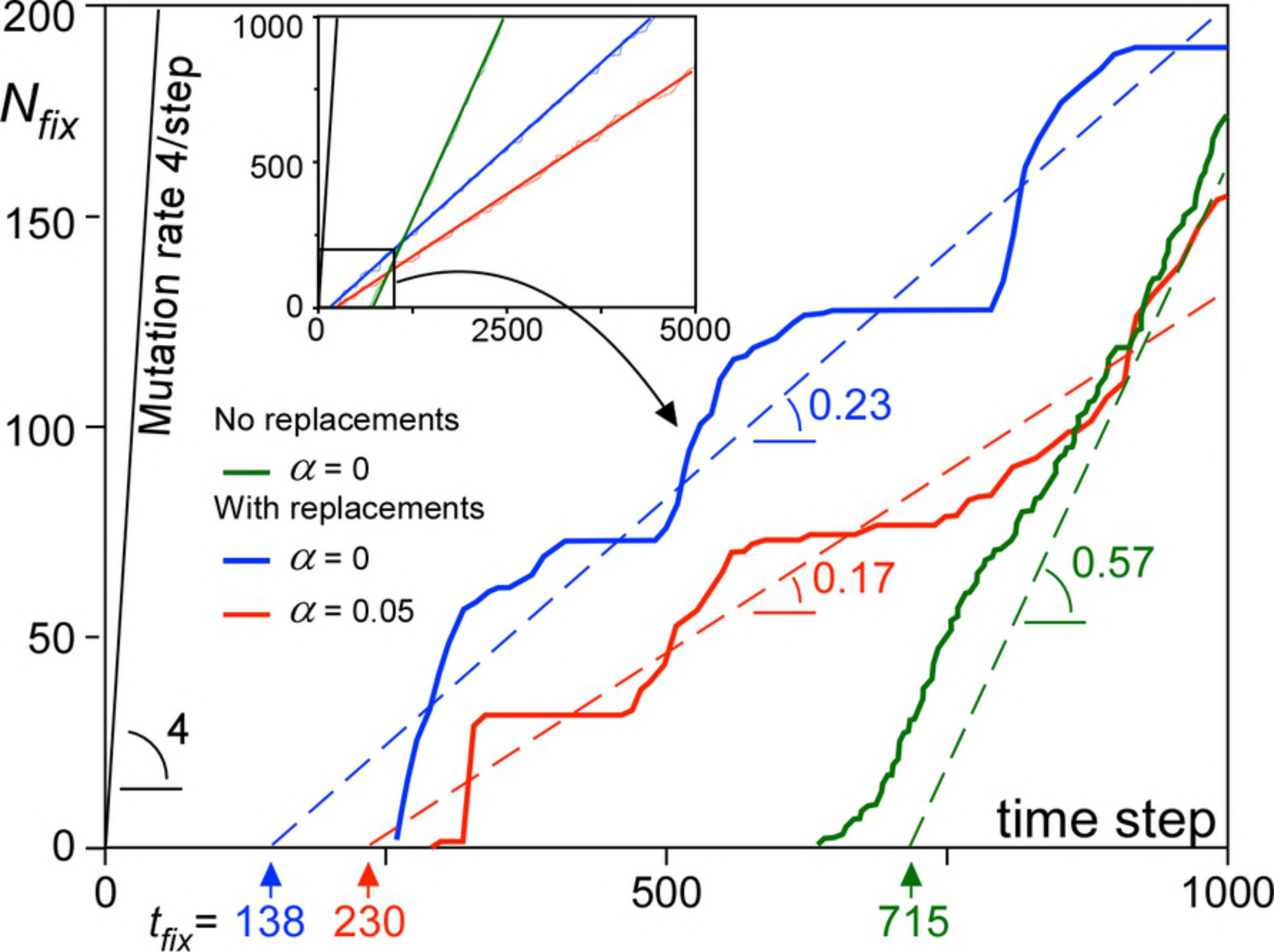
200
150
100
50
0
N_{fix}
Mutation rate 4/step
4
1000
500
0
0
2500
5000
No replacements
$\alpha = 0$
With replacements
$\alpha = 0$
$\alpha = 0.05$
0.23
0.17
0.57
time step
0
500
1000
t_{fix}= 138
230
715

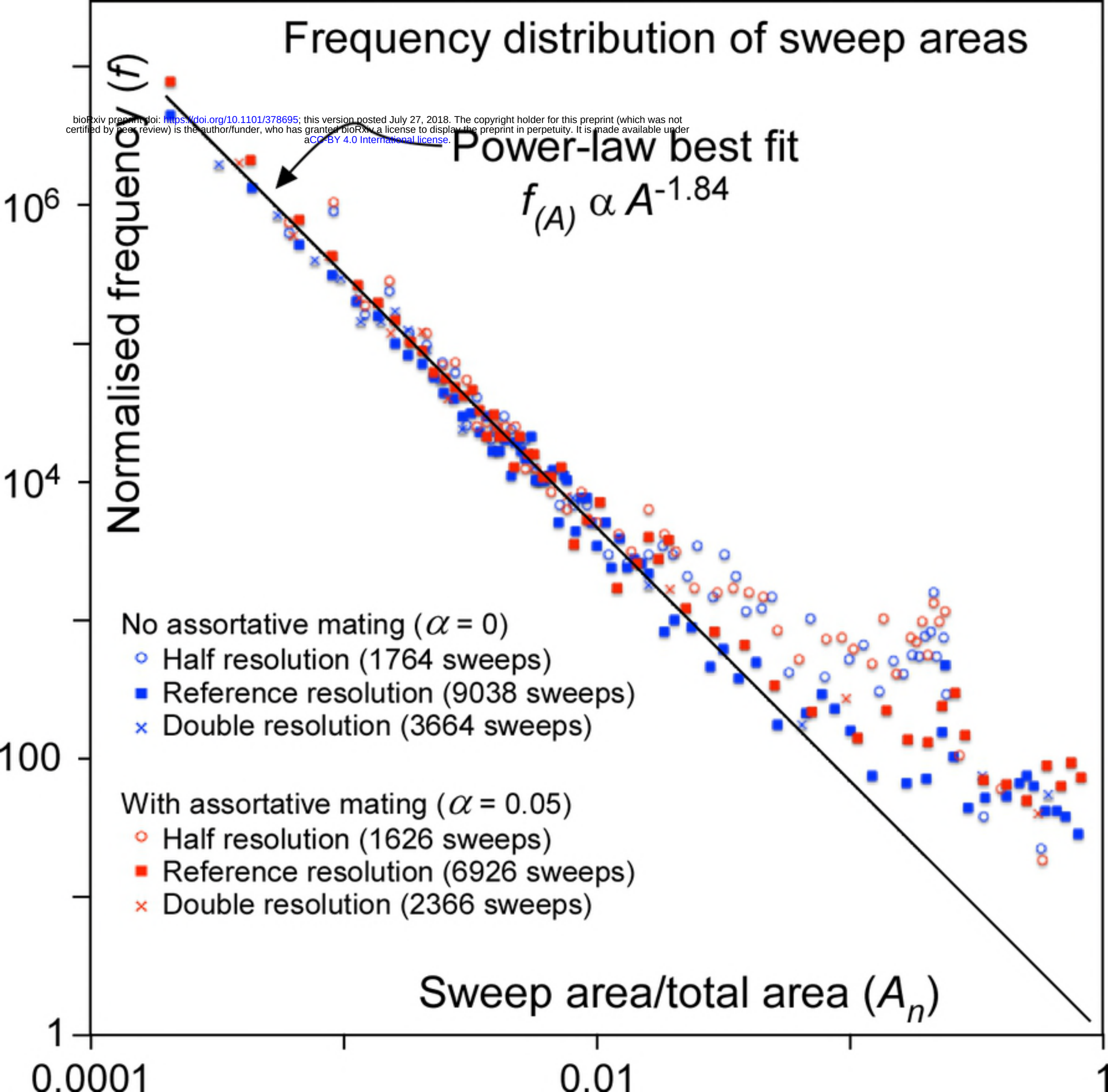

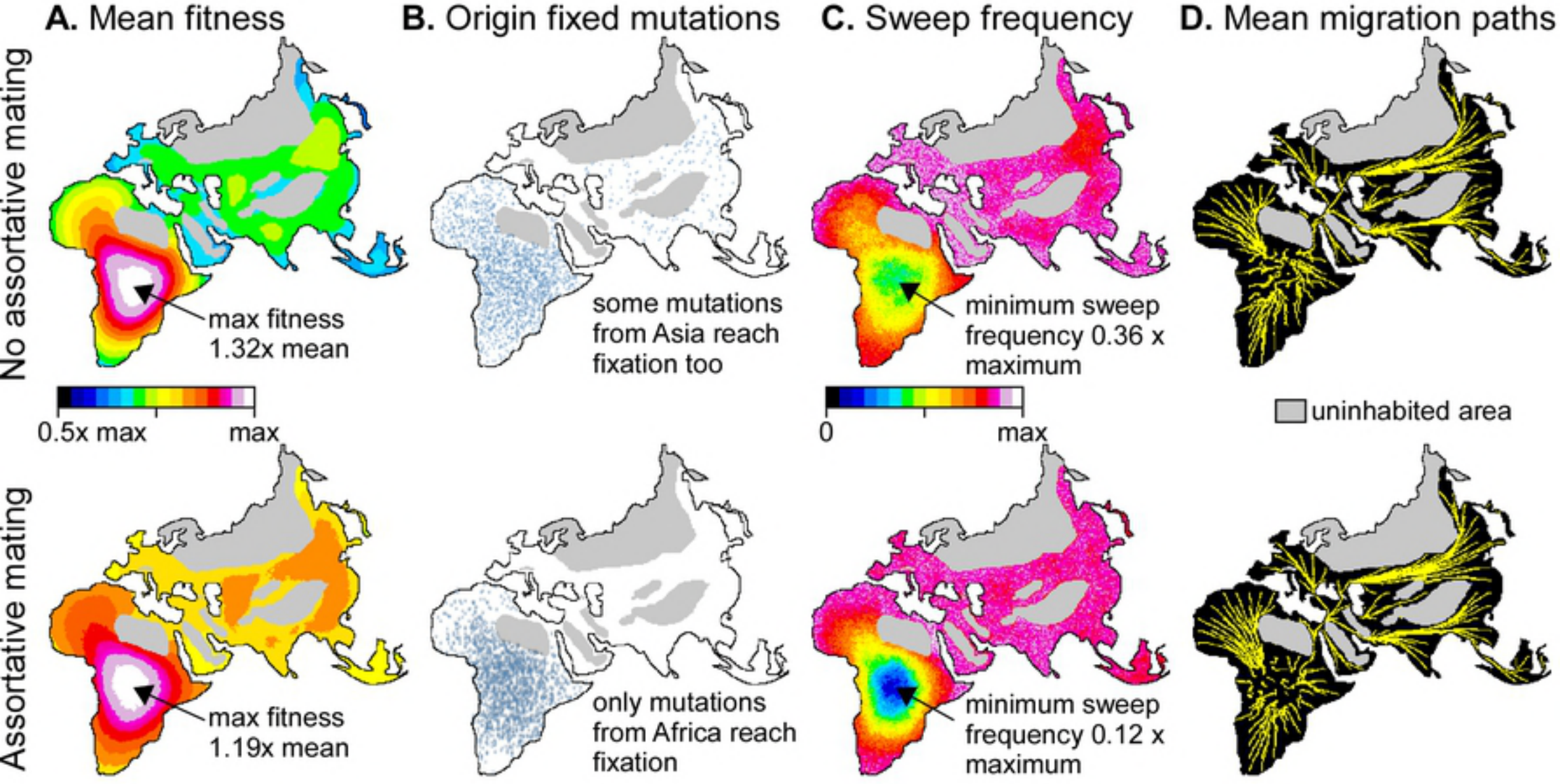
A. Mean fitness
B. Origin fixed mutations
C. Sweep frequency
D. Mean migration paths
No assortative mating
Assortative mating
max fitness
1.32x mean
some mutations
from Asia reach
fixation too
minimum sweep
frequency 0.36 x
maximum
0.5x max
max
0
max
uninhabited area
max fitness
1.19x mean
only mutations
from Africa reach
fixation
minimum sweep
frequency 0.12 x
maximum

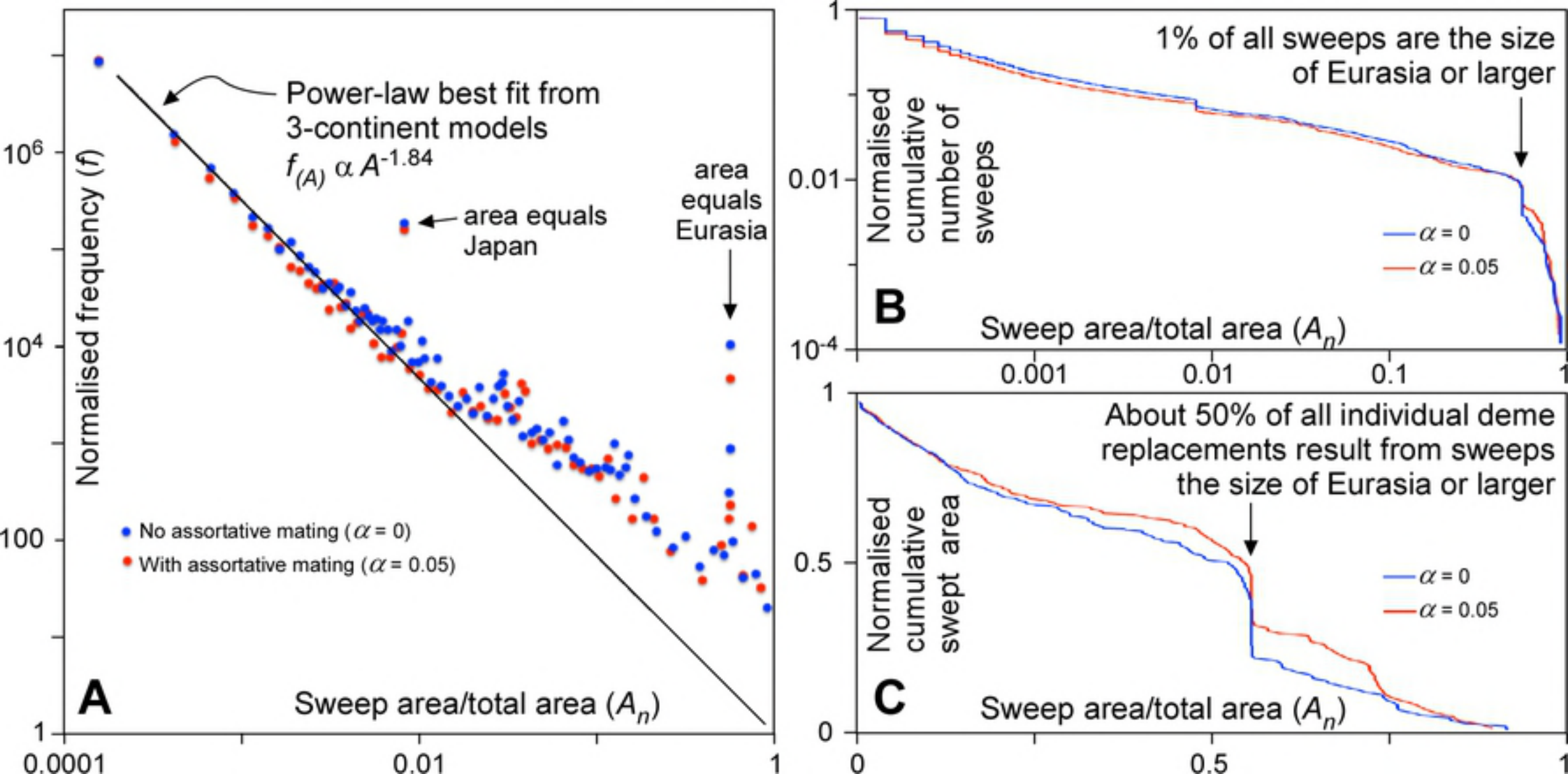
Power-law best fit from 3-continent models
$f_{(A)} \propto A^{-1.84}$
area equals Japan
area equals Eurasia
Normalised frequency (f)
No assortative mating ($\alpha = 0$)
With assortative mating ($\alpha = 0.05$)
A
Sweep area/total area (A_n)
1% of all sweeps are the size of Eurasia or larger
Normalised cumulative number of sweeps
B
About 50% of all individual deme replacements result from sweeps the size of Eurasia or larger
Normalised cumulative swept area
C